Available online at www.sciencedirect.com
ScienceDirect
Journal of Applied Geophysics 60 (2006) 213–224
JOURNAL OF APPLIED GEOPHYSICS
www.elsevier.com/locate/jappgeo

Azimuthal resistivity soundings over a steeply dipping anisotropic formation
A case history in central Tunisia

M. Schmutz [a,*], P. Andrieux [b,1], A. Bobachev [c,2], J.P. Montoroi [d,3], S. Nasri [e,4]

[a] University Bordeaux 3, EGID Institute, 1 allée Daguin, 33607 Pessac cedex, France
[b] University Paris 6, UMR Sisyphe, Paris, France
[c] Moscow State University, Geological Faculty, Department of Geophysics, Moscow, Russia
[d] Institut de Recherche pour le Développement, Geovast, Bondy, France
[e] Institut National de Recherche en Génie Rural, Eaux et Forêts, rue Hédi Karray, BP 10, Ariana, Tunisia

Received 31 August 2005; accepted 11 May 2006

Abstract

Azimuthal Resistivity Soundings (ARS), using the so-called "Arrow-type array" as proposed by Bolshakov et al. were carried out in Central Tunisia, together with azimuthal resistivity tomography, because of the known anisotropic behaviour of the nearly vertical formations.

First, the developments designed by Bolshakov et al. are reviewed: they deal with the separation between the effects of anisotropy and of heterogeneities, the design of the Arrow-type array and the introduction of the azimuthal spectral analysis.

Second, the main methodological results obtained near Gouazine Lake are presented: (1) the clear effect of a quasi-vertical contact and (2) the characterisation of the anisotropic substratum below a thin superficial layer in one site close to the axis of the valley: the strike direction ($\alpha = 50°$N), and a rather high anisotropy coefficient ($\lambda \approx 4$) are determined.

And lastly two directions for further developments are suggested.

Keywords: ARS (azimuthal resistivity sounding); Anisotropy; Tunisia; Direct current

1. Introduction

Direct current measurements and specifically electrical tomography today, are of great help to geologists and hydrogeologists for detailed subsurface mapping. In specific situations however, it has been found that the best match between borehole data and results of joint inversions of DC and TDEM soundings required the introduction of high value anisotropy coefficients (Schmutz et al., 2000).

Shallow low induction frequency domain electromagnetics and DC measurements were planned to be used in central Tunisia, near Gouazine Lake, for hydrogeological and soil investigations. Since the geological formations were known to be anisotropic and strongly dipping in the studied area, it was decided to apply two of the new techniques in electrical prospecting

* Corresponding author. Tel.: +33 5 5712 1016; fax: +33 5 5712 1001.
E-mail addresses: schmutz@egid.u-bordeaux.fr (M. Schmutz), ep_andrieux@infonie.fr (P. Andrieux), boba@geophys.geol.msu.ru (A. Bobachev), Jean-Pierre.Montoroi@bondy.ird.fr (J.P. Montoroi), nasri.slah@iresa.agrinet.tn (S. Nasri).
[1] Tel.: +33 1 4427 4828; fax: +33 1 4427 5125.
[2] Tel./fax: +7 95 939 49 63.
[3] Tel.: +33 1 4802 5533; fax: +33 1 4847 3088.
[4] Tel.: +216 71 717801; fax: +216 71 71951.

0926-9851/$ - see front matter © 2006 Elsevier B.V. All rights reserved.
doi:10.1016/j.jappgeo.2006.05.003

dedicated to studying such specific and complex situations.

The two techniques and arrays that were tested are (i) conventional azimuthal electrical tomography and (ii) Azimuthal Resistivity Soundings (ARS) using the Arrow-type array as proposed by Bolshakov et al. (1998a,b). The first technique was meant at studying the homogeneity of the environment at selected stations and delivering detailed images of the potentially 2D and 3D situations. The second one was an attempt at characterizing the anisotropic substratum under favourable conditions, at those same stations.

The objective and the main contribution of this presentation are mainly methodological. They are twofold:

- First a synthetic review of the state of the art in studying anisotropic formations in electrical prospecting is presented. It starts from the pioneering work by Maillet (1947), confined to studying one dimensional situations. Then the work by Habberjam (1972, 1975) is introduced. He was first to study the case of a half-space made up of a pile of tilted thin alternatively conductive and resistive beds and he proposed the use of the "square array". Lastly, a brief review of the thorough work carried out at the university of Moscow by Bolshakov et al. (1995, 1997, 1998a,b) is presented. The Arrow-type array as proposed by these authors, which we have used in central Tunisia is described with some details. A full description of their work can be found on their site: http://www.geol.msu.ru/deps/geophy/rec_lab2.htm.
- Second, in the last part of this presentation, the qualitative and quantitative results obtained in central Tunisia, by using these two specific techniques are presented. This is indeed one of the main interest of this presentation: a case history where field work and quantitative results obtained by the use of the Arrow-type array at two specific stations near Gouazine Lake are described, discussed and compared to the results obtained by azimuthal resistivity tomography.

2. Studying homogeneous anisotropic geological formations in direct current prospecting

Anisotropy was introduced at the very beginning of electrical prospecting by Maillet (1947). He was then mainly referring to sedimentary formations, i.e. clays and marls with horizontal bedding. Their electrical properties are understandably different when the current is flowing parallel or perpendicular to the bedding (Fig. 1a). The classical four parameters were introduced at that time: (1) ρ_l the longitudinal resistivity, (2) ρ_t the tranversal resistivity, (3) $\rho_m=(\rho_l\times\rho_t)^{1/2}$ the average resistivity and (4) $\lambda=(\rho_t/\rho_l)^{1/2}$ the anisotropy coefficient. He then enlarged his concept to micro, macro and pseudo-anisotropy. At that time he was dealing exclusively with horizontally layered media, i.e. 1D situations. It was clear that such an anisotropy could not be detected from surface measurements only and the so-called "paradox of anisotropy" was discovered, referring to measurements carried out in vertical boreholes at that time.

Habberjam (1972, 1975) was first to study in detail the case of a homogeneous half-space, made up of a pile of tilted thin beds as shown on Fig. 1b. Such an anisotropic formation may still be characterized by the same four parameters as above (ρ_l, ρ_t, ρ_m, and λ), but the strike azimuth (β) and the dip of the bedding (α) must also be considered.

At a surface point P, at a distance r from a surface source O, where OP makes an angle φ with the strike direction, the electric potential is shown to be equal to:

$$V(r,\varphi)=\frac{I\rho_m}{2\pi r\sqrt{1+(\lambda^2-1)\sin^2\alpha\sin^2\varphi}} \quad (1)$$

It is clear again, that from surface measurements:

- only "apparent parameters" can be "measured": ρ_{amax}, ρ_{amin}, ρ_{am} et $\lambda_a=(\rho_{amax}/\rho_{amin})^{1/2}$ and that the paradox of anisotropy applies, so that ρ_{amax} is obtained when the current is flowing parallel to the strike;
- α and λ cannot be separated, so that the so-called "effective anisotropy coefficient" must be introduced:

$$\lambda_{eff}=(1+(\lambda^2-1)\sin^2\alpha)^{1/2} \quad (2)$$

with $1\le\lambda_{eff}\le\lambda$.

Bolshakov et al., (1995, 1997, 1998a,b) have thoroughly studied the overall problem of direct current prospecting above anisotropic formations. They have covered most aspects of the topic and have introduced new concepts and new tools for practical applications:

(1) Their terminology has to be clearly understood and followed very strictly:

The term "anisotropy" applies strictly to characterize one geological formation by itself: one layer or possibly one substratum is anisotropic when it is made up of a pile of thin beds of different specific true resistivities; it is thus characterised by its own six parameters as introduced above (Fig. 1b). Such an anisotropic formation can be incorporated into a 1D, a 2D or a 3D model.

The term "inhomogeneity" for the authors, refers to the whole structure; it applies to 2D or 3D models, as opposed

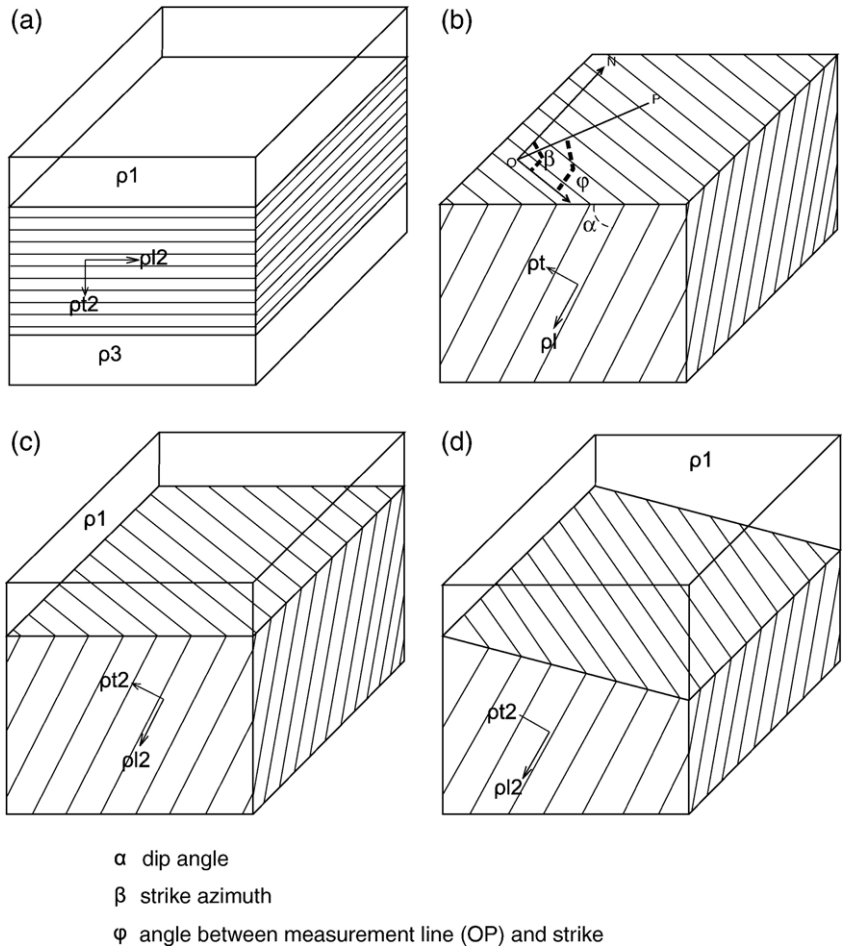

Fig. 1. Typical simple anisotropic and/or heterogeneous models: a: one anisotropic layer with horizontal bedding within a one dimensional model. b: one half-space made up of an infinitely thick tilted anisotropic formation. c: one isotropic horizontal layer on top of an anisotropic substratum (anisotropy but no heterogeneity). d: one dipping interface separating one isotropic surface layer and an anisotropic substratum (anisotropy plus heterogeneity).

to layered earth models. They clearly separate the case of the presence of one or more anisotropic layer with non-horizontal bedding, incorporated into an otherwise 1D model, from one of a 2D or 3D model, with or without the presence of anisotropic formations:

A. In the first situation (Fig. 1c), at the surface of the earth, apparent resistivity values will exhibit variations relative to the orientation of the array, but they will be the same for all stations, whatever their location.
B. In the second situation (Fig. 1d), on the other hand, resistivity values will vary relative to the orientation of the array at each station and at the same time, they will vary from one station to another, according to their location relative to the non-horizontal boundaries between the formations.The authors also acknowledge the fact that in real life, the second situation often prevails, i.e. effects of anisotropy of specific formations and of 2D or 3D effects are generally superimposed. Their objective is to separate these two effects and to enhance the influence of anisotropy, in order to recognize it for sure and to introduce the correct parameters into quantitative interpretation, in order to get a model as close as possible to reality.

(2) They have developed forward modelling capabilities and applied them to simple cases for both situations described above, for all classical arrays and for new specific ones devoted to enhance the influence of anisotropy relative to the existence of 2D and 3D effects, as mentioned earlier. Comparisons of sensitivity of various arrays have led them to the design of the so-called Arrow-type array described below and applied in central Tunisia. No inversion programs are available yet.

(3) They have introduced the concept of "azimuthal spectrum" of the apparent resistivity polar diagrams calculated and drawn for successive orientations of any array with given basic dimensions. As expected from the previous discussion, the two situations (A and B) will be separated by the morphology of those polar diagrams: the first situation will lead to symmetrical diagrams, whereas the second one will lead to asymmetrical ones. As a consequence, the spectrum in the first case will contain even harmonics only, whereas the second one will exhibit even and odd harmonics. This is one qualitative and quantitative means of separating the two effects, at one single station.

Some recent publications covering model studies and field results confirm most of those results described above for crossed square arrays (Senos Matias, 2002), as well as for classical linear arrays (Busby, 2000), or for 5-electrode offset Wenner array (Watson and Barker, 2005).

3. The arrow-type array and the azimuthal spectral analysis

Historically, the classical linear arrays (Wenner and Schlumberger) were first used to carry out Azimuthal Resistivity Soundings (ARS), in order to demonstrate and possibly to characterize the existence of non-horizontal bedding. With such arrays however, it is impossible to differentiate between the presence of tilted anisotropic formations within otherwise 1D situations and 2D or 3D effects related to fracturation or to tectonics, since polar diagrams are always symmetrical.

The square array was first introduced (Habberjam and Watkins, 1967), in order to minimize the effects of anisotropy or heterogeneity by spatial averaging. It was later proposed for strike determination (Habberjam, 1972, 1975) and anisotropy characterisation (Senos Matias, 2002).

The equatorial dipole array was recommended as early as 1975 by Semenov; as exhibiting a higher apparent sensitivity to anisotropic situations, compared

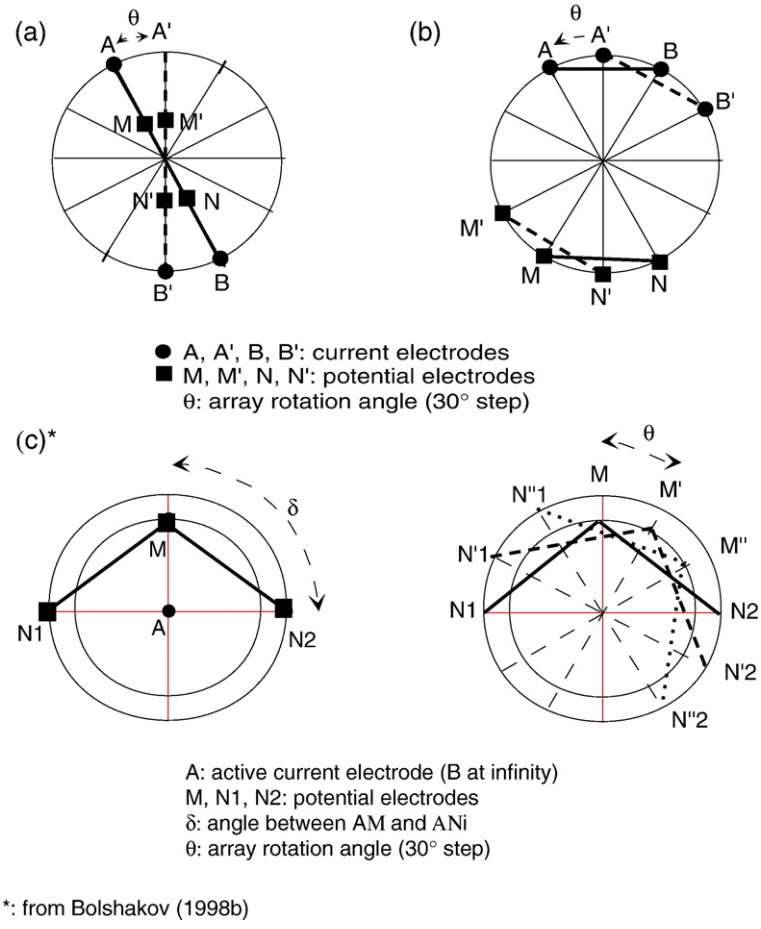

Fig. 2. Three different azimuthal resistivity arrays: a: The Wenner array. b: The equatorial dipole array. c: The Arrow Type array.

to linear arrays. New arrays were then searched for, to enhance this sensitivity, by combining measurements of two quasi-rectangular components of the electric field. The Arrow-type array was finally proposed by Bolshakov et al. (1998a), which does show a higher sensitivity to anisotropy, plus additional useful properties as it will be described below.

An example of a typical configuration, for a 30° rotation step, is shown on Fig. 2c, adapted from their publication and compared to a classical Wenner array (Fig. 2a) and to the equatorial dipole (Fig. 2b). The measurement procedure is as follows: A is the central transmitting electrode (B is at infinity). Two independent potential differences are measured : $V_M - V_{N1}$ and $V_M - V_{N2}$. The array is then rotated by an angle of 30° and the same measurements apply. This is repeated for successive rotation angles of 30°. The depth of investigation is related to AO=(AM+AM)/2. A sounding is classically carried out by increasing the distance AO step by step. A multi-electrode acquisition system is well adapted to carrying out such soundings.

The very high intrinsic sensitivity to anisotropy may be measured by the ratio λ_a/λ, where λ_a is classically defined as above: $\lambda_a=(\rho_{amax}/\rho_{amin})^{1/2}$. As shown on Fig. 3a, corresponding to the specific forward calculations for an anisotropic half-space with $\lambda=2$, this ratio might be as high as infinity since ρ_{amin} may be equal to 0. Moreover, when negative values of apparent resistivity are measured, as shown again on Fig. 3a and b, a slightly modified definition of λ_a is applied. Two possibilities are proposed: $\lambda_a=(\rho_{amax}/\rho_{amin})^{1/2}$. Eq. (2) may be replaced either by

$$\lambda_a = [1 + (\rho_{amax} - \rho_{amin})/|\rho_{amin}|)]^{1/2} \quad (3)$$

or by

$$\lambda_a = [1 + (\rho_{amax} - \rho_{amin})/\rho_{amax})]^{1/2}. \quad (4)$$

Regarding the array itself, its specificities are as follows (Fig. 2c):

- the use of a single source pole (B is at infinity), which is more relevant than a dipole source for rotation,
- the inequality, AM<AN which ensures a non-zero potential difference over a horizontally layered model,
- the symmetry of MN_1 and MN_2 relative to AM, which enables to detect near surface or deep heterogeneities; as opposed to anisotropy,
- a rather "narrow" azimuthal spectrum, which means that the amplitude of the fourth harmonic is quite small compared to the fundamental and/or the first one, i.e. that an azimuthal step of 45° would theoretically be sufficient (30° is proposed however),
- a rather simple logistics in the fields, since the array is built up from two lines at right angle to each other with equidistant electrodes along each of them,
- a simple and quick procedure to carry out soundings with a multi-electrode acquisition system.

Regarding data processing, they propose the azimuthal spectral analysis of polar diagrams, which also shows distinct advantages:

- it enables to reconstruct the response of any array, including the classical linear arrays (Wenner/Schlumberger), from the one which has been used in the fields, when spatial sampling is adequate,

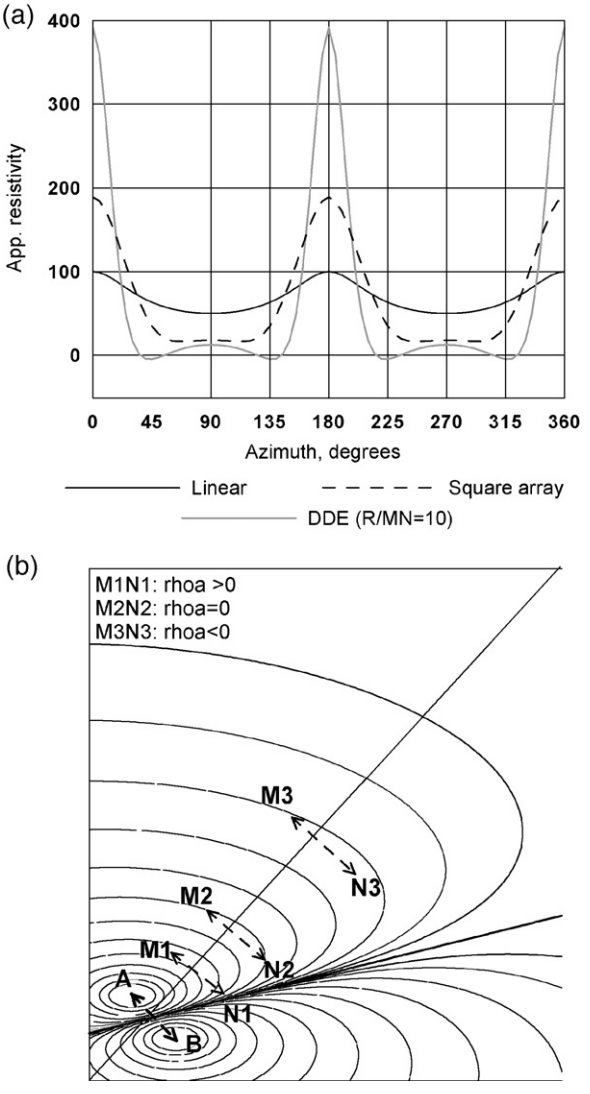

Fig. 3. Apparent sensitivity of different arrays. a: $\rho_a=f(\theta)$ for linear, equatorial dipole and square arrays. b: Isopotential lines for equatorial dipole array to explain negative apparent resistivity values.

– it leads to robust equations for all classical anisotropy parameters,
– it enables, at single stations, to separate between the presence of anisotropic formations versus 2D or 3D effects, through the use of the ratio between the sums of odd and even harmonics.

The case history below shows one practical example of this approach, together with more classical azimuthal tomography measurements.

4. Application near Gouazine Lake, Central Tunisia

Gouazine Lake is one of numerous artificial water reservoirs built in Tunisia for agricultural purposes. It is located approximately 110 km SW of Tunis and 50 km NW of Kairouan (Fig. 4).

The geophysical survey discussed thereafter is part of a large project initiated by hydrogeologists and soil scientists from France and Tunisia (Montoroi et al., 2000). Its objective was to help understanding the impact of the dam and of the lake on water circulation and on neighbouring soils, for which an increase in salinity was especially feared.

The geological environment is rather complex; no detailed geological map is available (only 1/200 000 scale). The study area is located to the northwest of an Oligocen dated basin, at the eastern edge of the Ousseltia syncline. The general structural orientation is NE–SW. Strongly dipping thin beds showing alternating limestones, marls and sandstones dated from Eocen to Oligocen are clearly outcropping around the lake, as well as in the surrounding area. The dam is built across a small valley; which is cut within fine and coarse grain quaternary deposits.

The objective of the geophysical survey was threefold :

(i) to map conductivity anomalies within the quaternary deposits in the small valley, that might be related to increasing salinity of the soils,
(ii) to map the bedrock below the valley in selected places, to discover potential features of importance for water circulation,

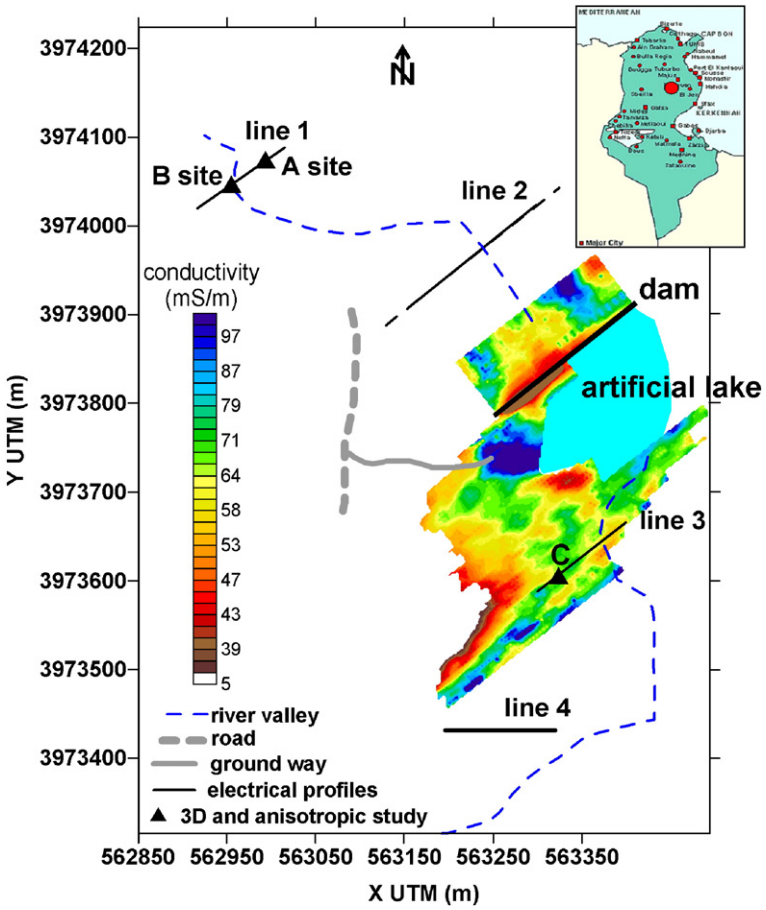

Fig. 4. Geophysical survey near Gouazine Lake (Central Tunisia): Location map and results of shallow electromagnetic conductivity mapping.

(iii) to test two of the newly developed DC techniques to be used in complex geology areas.

4.1. Data acquisition

The overall geophysical program (Fig. 4) consisted in three successive tasks:

(i) Low frequency electromagnetic mapping, using a Geonics EM 31 equipment: the so-called "Vertical Magnetic Dipole" configuration was used. A regular grid with a 5 m spacing was set up; 2 days were devoted to acquiring the whole data set; the field conditions were quasi-ideal: open space, no vegetation and little topography.

(ii) Reconnaissance electrical tomography (Loke and Barker, 1996) along 4 lines (line1 to line 4): the Wenner α configuration was used systematically, Wenner β was carried out in most places too. Basic spacing "a" was equal to 4 m, with 64 electrodes for the longest array, i.e. AB max=3 a=252 m. Field conditions were rather difficult for electrical measurements because of generally high resistivity surface material. The amplitude of the signal was the limiting factor in terms of depth of exploration, especially for Wenner β configuration.

(iii) Detailed studies of anisotropy/heterogeneity at 3 selected sites (A and B on line 1 and C on line 4), using the two techniques mentioned above : (i) electrical tomography using Wenner α and β configurations again and (ii) Arrow-type array soundings. The inter-electrode spacing along each set of rectangular diameters was the same for both types of arrays — Wenner and Arrow-type. It was equal to 1 m for sites A and B and equal to 2 m for site C. For that same site C, the maximum dimension for each array was thus equal to AB max=3 a=60 m (Wenner α) and AM=28 m whereas AN1=AN2=30 m (Arrow-type). Since the same azimuthal step equal to 30° was deliberately chosen for both techniques, the same electrode set up was used successively for each technique. Thanks to the specific multi-electrode equipment from Iris Instrument and to pre-registered sequences, both types of measurements were acquired extremely rapidly along each set of rectangular diameters. Again, because of open space and lack of vegetation, rotating the arrays by 30° was a rather easy task.

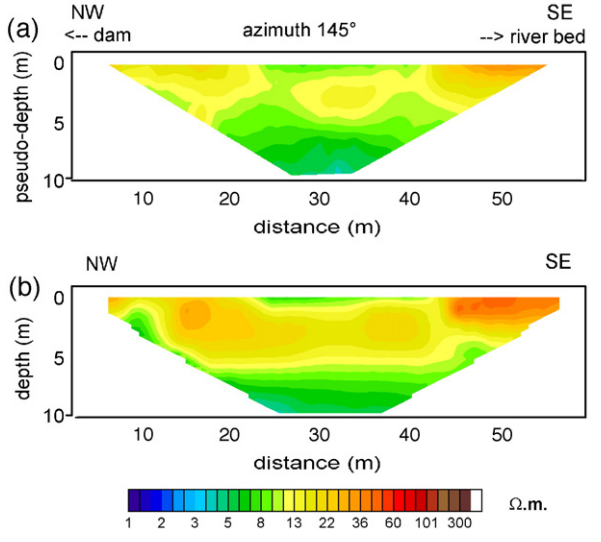

Fig. 5. Line 3 — SiteC — Example of one detailed resistivity tomography section.

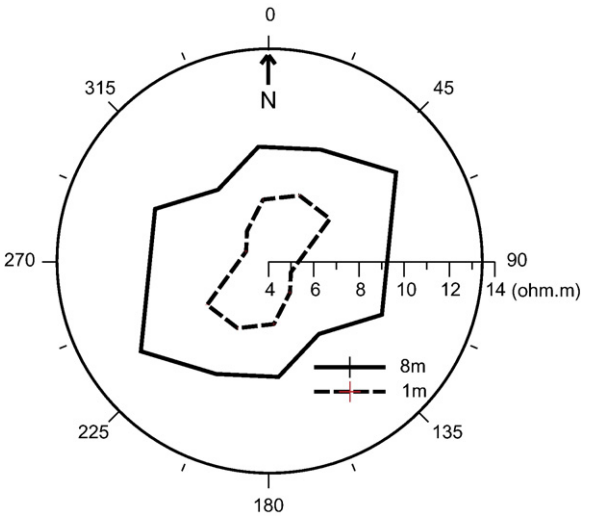

Fig. 6. Line 3 — SiteC — Two polar diagrams from Wenner α array.

4.2. Results

4.2.1. Electromagnetics: the conductivity map

Three conductive anomalies — three blue patches on the map — are clearly visible close to the dam — one upstream and two downstream. This unexpected and new information has led to soil sampling at depths of approximately 50 cm, which was unluckily too shallow to conclude whether these high conductivity values were related either to increasing porosity, higher salinity water or higher clay content. Deeper sampling is yet to be carried out (Fig. 4).

From this map and from field examination, line 3 has been selected, as one test area for studying the anisotropic behaviour of the substratum.

4.2.2. DC measurements — azimuthal tomography and arrow-type soundings for two sites

Inversion of electrical tomography sections has been carried out using RES2DINV (Loke and Barker, 1996). The maximum number of iterations was equal to 5; the order of magnitude of the RMS error after the last iteration was always smaller than 3%. As it will be shown below, the 1D/2D hypothesis did not apply for a number of azimuthal profiles for site A.

Regarding the Arrow-type soundings, the "classical" processing and interpretation schemes developed by Bolshakov et al. (1998a,b) could be applied with no restriction for site C.

This was not the case for site A.

4.3. Site C

The "true resistivity" cross-section obtained at site C from detailed tomography using the Wenner α configuration (Fig. 5), does show a quasi-horizontal layer situation: a three layer model with a moderately resistive one in the middle, seems relevant.

Two polar diagrams drawn from measured apparent resistivities with Wenner α configuration (Fig. 6) show two "pseudo-ellipses" for two different dimensions ($a=1$ and 8 m). Because the array is linear and symmetrical, the patterns are also symmetrical. The azimuth of the maximum axis is around 30°N for the small array ($a=1$ m), it is around 50°N for the larger one ($a=8$ m).

The results of the arrow-type array as expected, drastically emphasise the anisotropy situation, as demonstrated by the six successive polar diagrams drawn according to the conventions described above (Fig. 7). The strike direction appears rather stable with increasing depths of exploration, i.e. from $a=5$ m to $a=13$ m. It is of the order of 50°N. The experimental apparent resistivity diagrams are almost symmetrical, both for the positive and for the negative values. The amplitude ratio "Odd/Even" is rather low for the two larger arrays (0.29 and 0.21). All those features tend to prove that there seems to be no 2D or 3D effects superimposed to the anisotropic situation.

Direct modelling with a two layer model has thus been proposed: a thin isotropic top layer above an anisotropic substratum. The best fit between the experimental and synthetic data requires rather high values for λ_{eff} however. Because the minimum value of λ is obtained

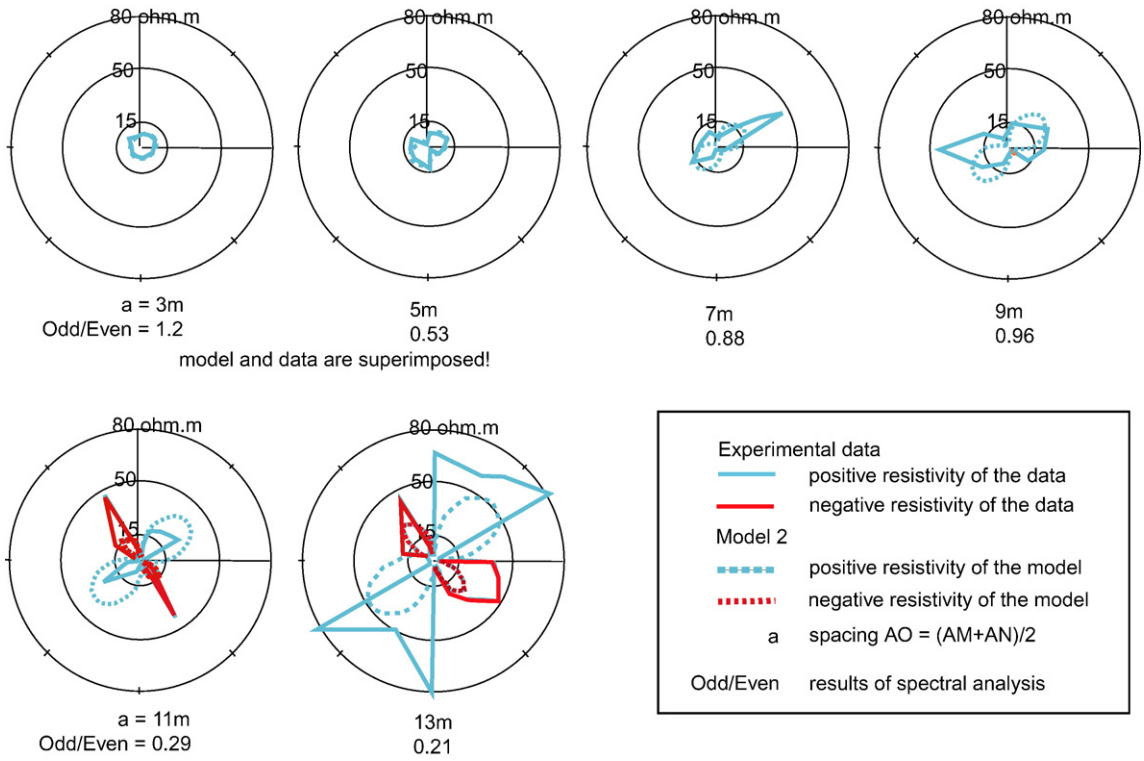

Fig. 7. Line 3 — SiteC — Results of the Arrow-type array measurements: experimental data and model polar diagrams for 6 increasing dimensions of the array.

Table 1
Site C — two anisotropic models compatible with ARS experimental data

Parameters	Model 1		Model 2	
	Layer 1	Layer 2	Layer 1	Layer 2
Minimal resistivity: ρ_{min} (Ω m)	7	7.5	4.3	15
Average resistivity: ρ_{ave} (Ω m)	7	30	4.6	30
Maximal resistivity: ρ_{max} (Ω m)	7	120	4.9	60
Dip: α (°)	none	90	90	90
Strike: β (°)	none	50	50	50
Anisotropy coefficient: λ	1	4	1.06	2
Thickness: h (m)	2	∞	1	∞

when sin α is equal to 1, i.e. when the dip value is equal to 90°, this dip value has been kept for the final interpretation. In other words, the hypothesis is proposed of a substratum made up of vertical thin beds. The "true" anisotropy coefficient however still remains extremely high (λ=4). Attempts have been made to lower this value. The only way consists in sharing anisotropy between the top layer and the substratum, by keeping the same strike direction for both formations; the upper layer thus becomes thinner, compared to model 1 (Table 1).

The similarity between the experimental and model 1 data is acceptable (Fig. 7); the main discrepancies are most probably due to electrode effects, the so-called "à coup de prises". This is the only way to explain the large increase in the experimental $\tilde{n}_a$ values when "a" increases from 11 to 13 m. The most striking feature is the appearance of significantly high negative apparent resistivity values when "a" increases above 9 m, both for the experimental and the model data.

Table 2
Site A — the "best" 2 layer anisotropic 1D model

Parameters	Layer 1	Layer 2
Minimal resistivity: ρ_{min} (Ω m)	7	7.5
Average resistivity: ρ_{ave} (Ω m)	7	30
Maximal resistivity: ρ_{max} (Ω m)	7	120
Dip: α (°)	none	90
Strike: β (°)	none	140
Anisotropy coefficient: λ	1	4
Thickness: h (m)	2	∞

It can be concluded that the data set acquired in site C with the Arrow-type array is compatible with a two layer model with a horizontal interface between a shallow surface layer and an anisotropic infinite substratum made up of vertical or nearly vertical thin beds. This model is in acceptable agreement with the known geology.

4.4. Site A

Results of the NE/SW reconnaissance resistivity tomography along line 1 (Fig. 8), clearly shows a non-horizontal layer situation, within the first 15 m thickness, around abscissas X=30 m and X=80 m. Sites A and B have thus been selected around these locations for detailed azimuthal resistivity tomography as well as for Arrow-type array soundings, as opposed to site C presented above, where horizontal layering prevailed. Site A only is discussed thereafter (Table 2).

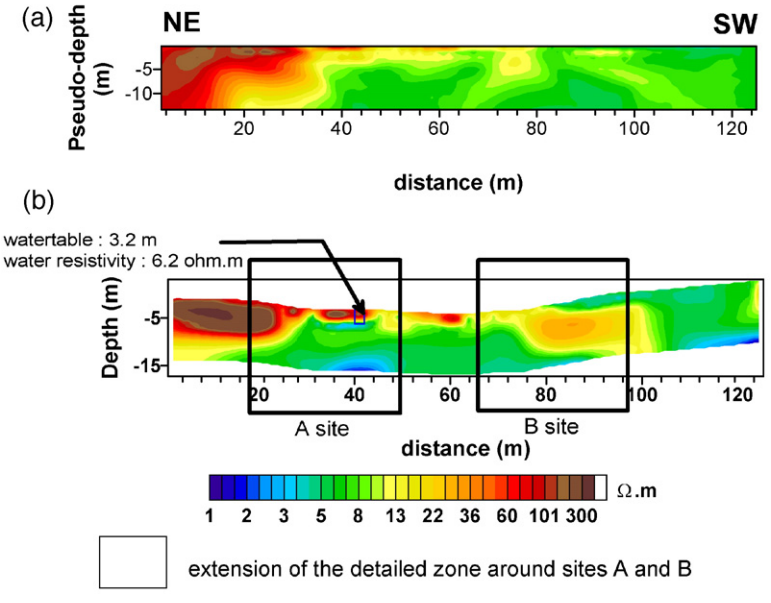

Fig. 8. Line 1 — Results of reconnaissance resistivity tomography.

As a result of the inversion of detailed tomography measurements using RES2DINV software, seven cross-sections are shown (Fig. 9); they are labelled (a) to (g) from top to bottom. Two clear features can readily be recognized: (1) the existence of a quasi-vertical boundary which separates each profile into two domains and (2) the different "true resistivity" values at depth, on each side of this major feature, from one section to another. It must be stressed however that the 2D hypothesis applies solely for sections (c), (d) and (e) where the profiles are nearly at right angle to the contact; it is not the case for sections (a) and (b) and (f) and (g) where they are nearly parallel to the contact; it is clear also that (a) and (g) are mirror images one to the other. A quick look at those seven sections shows that true resistivity values appear to be maximal (>300 Ω m) for the terraces, for sections (c) and (e) and that they appear to be minimal (<3 Ω m) in the valley, for section (c).

From the Arrow-type measurements, six polar diagrams have been plotted (Fig. 10 — experimental data). Three features can be recognized: (1) a generally NNW/SSE trend of the major axis of the "pseudo-ellipses", (2) a clear dissymmetry of the lobes of the major pseudo-ellipses: higher resistivity values to the

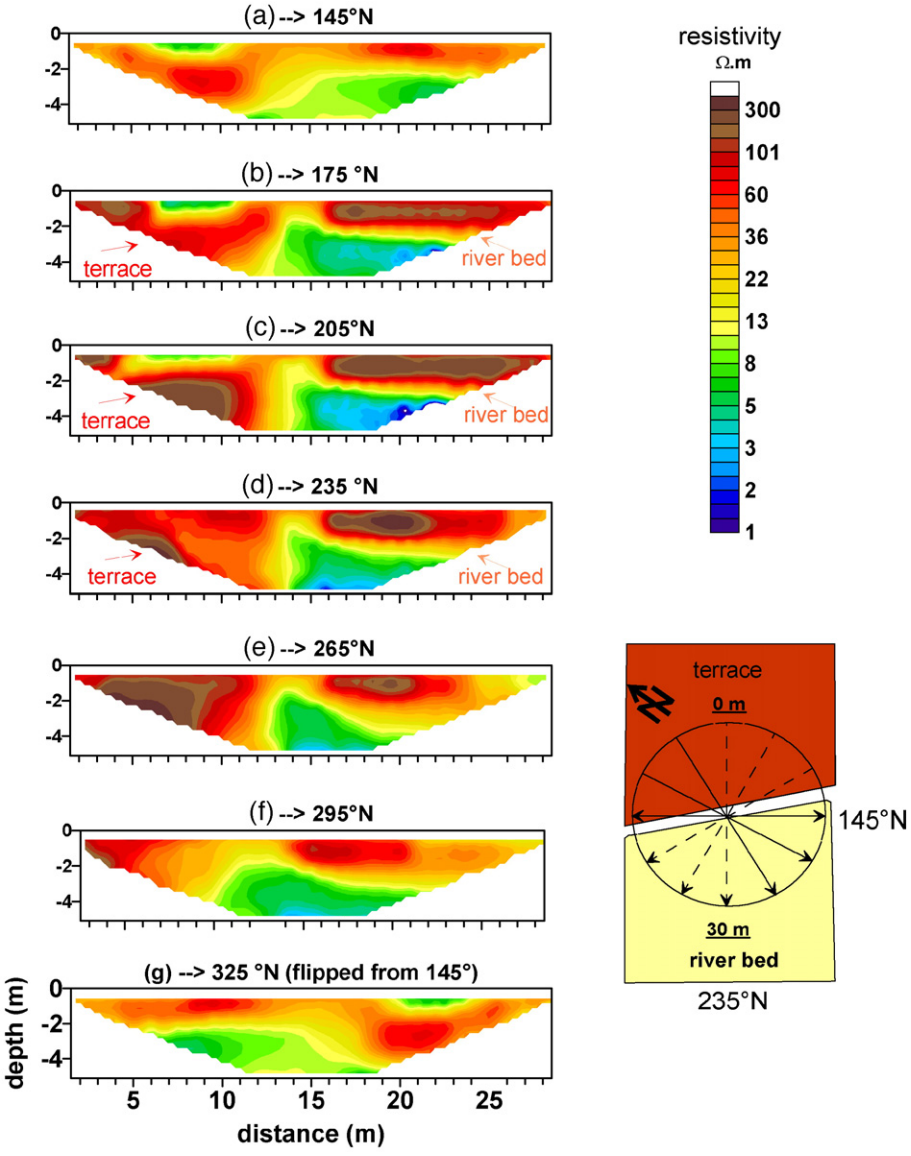

Fig. 9. Line 1 — Site A — Results of detailed azimuthal resistivity tomography.

South for the first two small arrays (a=2.5 and 4.5 m) whereas they are higher to the North–West for the larger arrays (a=8.5, 10.5 and 12.5 m) and (3) very high "Odd/Even" ratios for the two small arrays (2.3 and 1.3) and rather high ones for the larger ones also (0.74, 0.82 and 0.96). These features are clear signs of the very large influence of the quasi vertical WSW/ENE boundary, which separates the profiles into two different domains. Any intrinsic anisotropy of the formations on either side of the boundary is heavily masked by this major so-called heterogeneity.

Unfortunately at present, there are no 2D forward models available with a thin surface layer on top of an anisotropic substratum; on each side of a vertical contact. As a matter of comparison with site C however, the same model has been superimposed to the experimental data of site A, with a strike angle equal to 140°, as shown on Fig. 10. This strike angle is clearly related to the vertical contact between the two compartments. More work should clearly be done to try to separate between the effect of this contact and that of the anisotropic substratum; it is however rather puzzling to find out that there is an acceptable similarity between the experimental and model lobes in the north-western compartment for all six diagrams.

5. Conclusions and perspectives

The methodological objective set to this geophysical survey near Gouazine Lake has been reached to a large extent.

- It is proven that under favourable field conditions — open space with almost no vegetation — azimuthal resistivity tomography and azimuthal resistivity sounding using the Arrow-type array can efficiently be carried out, thanks to the use of multi-electrode acquisition systems.
- The Arrow-type array and its processing and interpretation procedures have proven to be able to separate between anisotropy and the presence of heterogeneity at three sites. At one of them it led to a reasonable quantitative characterisation of the anisotropic substratum below a thin surface layer.
- The limitations regarding quantitative interpretation have however been reached for the two techniques. Undoubtedly 3D tomography arrays and inversion procedures would be more appropriate than 2D azimuthal resistivity tomography to fully characterize a 3D block at single stations. Similarly additional experience and more elaborate direct models are

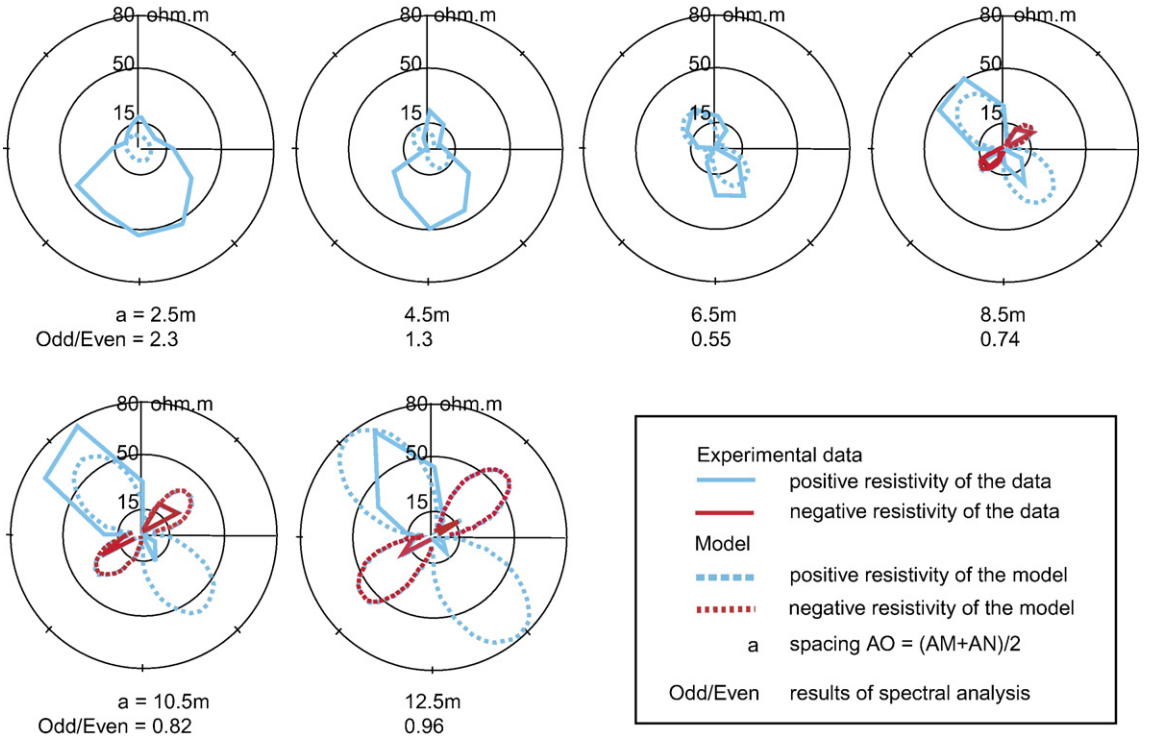

Fig. 10. Line 1 — Site A — Results of the Arrow-type array measurements: experimental and model polar diagrams for 6 increasing dimensions of the array.

required to fully interpret and exploit the results of Arrow-type soundings.

The objective set by the hydrogeologists and by the soil scientists to the geophysical investigation has also been reached to a large extent. The high density information contained in the conductivity map on one hand and the detailed images obtained along specific Lines and at single stations on the other hand, have proven to be valuable to locate control wells and trenches to better understand water circulation and for monitoring purposes.

Further to this first positive experiment, one can think of two developments of high academic and practical interests, which can be undertaken at once.

(1) Anisotropy should now be introduced into 2D and 3D numerical models in electrical tomography. There is little doubt that the presence of tilted anisotropic blocks into such models will modify the expected responses. Furthermore the inversion techniques already available in 3D tomography will be extremely valuable for ultimate quantitative interpretation.
(2) In the fields and on synthetic data, attempts at synthesizing the Arrow-type array from pole–pole measurements with adequate spacing between the electrodes is probably a direction of interest. All the processing and interpretation techniques specifically designed in the University of Moscow and partially tested in Tunisia should then be applied to such 3D resistivity data sets.

References

Bolshakov, D.K., Modin, I.N., Pervago, E.V., Shevnin, V.A., 1995. Anisotropy effects investigations by resistivity methods in some inhomogeneous media. 57th EAGE Conference, Glasgow, UK, Extended Abstracts, p. P034.

Bolshakov, D.K., Modin, I.N., Pervago, E.V., Shevnin, V.A., 1997. Separation of anisotropy and inhomogeneity influence by azimuthal resistivity diagram's analysis. Proceedings of the International Symposium on Engineering and Environmental Geophysics, Chengdu, China, pp. 239–245.

Bolshakov, D.K., Modin, I.N., Pervago, E.V., Shevnin, V.A., 1998a. New step in anisotropy studies: arrow-type arrays. Proceedings of the 4th EEGS-European Section Meeting, Barcelona, Spain, pp. 857–860.

Bolshakov, D.K., Modin, I.N., Pervago, E.V., Shevnin, V.A.n., 1998b. Modeling and interpretation of azimuthal resistivity sounding over two layered model with arbitrary oriented anisotropy in each layer. Proceedings of the AEGE 60th Conference, Leipzig, Germany, p. P110.

Busby, J.P., 2000. The effectiveness of azimuthal apparent resistivity measurements as a method for determining fracture strike direction. Geophysical Prospecting 48, 677–695.

Habberjam, G.M., 1972. The effects of anisotropy on square array resistivity measurements. Geophysical Prospecting 20, 249–266.

Habberjam, G.M., 1975. Apparent resistivity, anisotropy and strike measurements. Geophysical Prospecting 23, 211–247.

Habberjam, G.M., Watkins, G.E., 1967. The use of a square configuration in resistivity prospecting. Geophysical Prospecting 15, 445–467.

Loke, M.H., Barker, R.D., 1996. Rapid least-squares inversion of apparent resistivity pseudo-sections by a quasi-Newton method. Geophysical Prospecting 44 (1), 131–152.

Maillet, R., 1947. The fundamental equations of electrical prospecting. Geophysics 12 (4), 529–556.

Montoroi, J.P., Grünberger, O., Nasri, S., 2000. Caractérisation chimique et isotopique des eaux et des formations superficielles du bassin versant du lac collinaire d'El Gouazine (Tunisie centrale) Rapport scientifique de la campagne de mesure 1998. 107 pp.

Schmutz, M., Albouy, Y., Guérin, R., Maquaire, O., Vassal, J., Schott, J.J., et Descloîtres, M., 2000. Joint electrical and time domain electromagnetism (TDEM) data inversion applied to the Super Sauze earthflow (France). Surveys in Geophysics 21 (4), 371–390.

Semenov, A.S., 1975. Rock anisotropy and electrical field peculiarities in anisotropic media. Ser. Geol. and Geography, vol. 24. Vestnik of Leningrad University, pp. 40–47 (in Russian).

Senos Matias, M.J., 2002. Square array anisotropy measurements and resistivity sounding interpretation. Journal of Applied Geophysics 49, 185–194.

Watson, K.A., Barker, R.D., 2005. Modelling azimuthal resistivity sounding over a laterally changing resistivity subsurface. Near Surface Geophysics 3–11.